Supporting Information

High Mobility Transistors Based on Single Crystals of Isotopically Labelled Rubrene-d_{28}

Wei Xie[1], *Kathryn A. McGarry*[2], *Feilong Liu*[3], *Yanfei Wu*[1], *P. Paul Ruden*[3], *Christopher J. Douglas*[2] *and C. Daniel Frisbie*[1*]

[1]Department of Chemical Engineering and Materials Science, University of Minnesota, Minneapolis, Minnesota, USA, 55455

[2]Department of Chemistry, University of Minnesota, Minneapolis, Minnesota, USA, 55455

[3]Department of Electrical Engineering, University of Minnesota, Minneapolis, Minnesota, USA, 55455

*To whom it should correspond: frisbie@umn.edu

1. Synthesis Details

All reactions were carried out using flame-dried glassware under a nitrogen atmosphere. Tetrahydrofuran (THF) was dried by distillation from benzophenone/sodium. Dichloromethane (CH_2Cl_2) and triethylamine (TEA) were dried by distillation from CaH_2 under nitrogen. All other chemicals were purchased from Acros Organics or Sigma-Aldrich and used as received unless otherwise noted.

Analytical thin layer chromatography (TLC) was carried out using 0.25 mm silica plates from Silicycle. Eluted plates were visualized first with UV light. Flash chromatography was performed using 230–400 mesh (particle size 0.04–0.063 mm) silica gel purchased from Silicycle. ^{1}H NMR (300 MHz), ^{13}C NMR (75 MHz), ^{2}H (46.1 MHz) spectra were obtained on Varian FT NMR or Bruker FT NMR instruments. NMR spectra were reported as δ values in ppm relative to chloroform for ^{1}H (7.26 ppm), chloroform for ^{13}C (77.00 ppm), and dichloromethane-d_2 for ^{2}H (5.30 ppm). ^{1}H and ^{13}C NMR coupling constants are reported in Hz; multiplicity was indicated as follows; s (singlet); d (doublet); t (triplet); q (quartet); quint (quintet); m (multiplet); dd (doublet of doublets); ddd (doublet of doublet of doublets); dddd (doublet of doublet of doublet of doublets); dt (doublet of triplets); td (triplet of doublets); ddt (doublet of doublet of triplets); app (apparent); br (broad).

Deuterium incorporation was calculated as follows.[1] To an NMR tube was added: rubrene-d_{28} (9.5 mg, 0.0170 mmol), trimethoxybenzene (1.1 mg, 0.0065 mmol), followed by $CDCl_3$ (0.7 mL). The ^{1}H NMR spectrum was collected (500 MHz, 48 scans). Integration of the peaks for rubrene-d_{28} (1.65, 0.804, 1.00 per hydrogen for each peak respectively) and the internal standard (47.06 per hydrogen) were calculated. The residual mmol of hydrogen was calculated for each peak (ex. 1.65 / 47.06 × 0.0065 = 0.000228 mmol H) then converted into a percentage

(ex. 0.000228 / 0.0170 × 100 = 1.34%). The percent deuterium was calculated for each peak (ex. 100 – 1.34 = 98.6% deuterium) then the percentages were multiplied together to determine the overall deuterium incorporation (97.2%).

Infrared (IR) spectra were obtained as films from CH_2Cl_2. Low-resolution mass spectra (LRMS) in EI experiments were performed on a Varian Saturn 2200 GC-MS system. High-resolution mass spectra (HRMS) in EI experiments were performed on a Finnigan MAT 95 GC-MS system. Elemental analysis was performed by Atlantic Microlab, Inc., 6180 Atlantic Blvd, Suite M, Norcross, GA 30071.

(2,2-dibromovinyl)benzene-d_5[2]

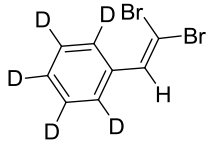

To a solution of zinc dust (4.31 g, 66.0 mmol), triphenylphosphine (17.31 g, 66.0 mmol) in 120 mL CH_2Cl_2, was added carbon tetrabromide (21.9 g, 66.0 mmol). After 24 hours of stirring at room temperature, benzaldehyde-d_5 (3.70 g, 33.0 mmol) was added. The mixture was stirred for 2 hours, then the solvent was removed *in vacuo*. Residue was subjected to multiple washes with a CH_2Cl_2/pentane solution (1:4). The solution was filtered and solvent removed *in vacuo* gave crude product. Purification by column chromatography using 3:2 hexanes:CH_2Cl_2 provided (2,2-dibromovinyl)benzene-d_5 as a light yellow oil (7.75 g, 29.3 mmol, 89%). R_f = 0.74 (3:2 hexanes:CH_2Cl_2); ^{1}H NMR (300 MHz, $CDCl_3$) δ 7.49 (s, 1 H); ^{2}H NMR (46.1 MHz, CH_2Cl_2) δ 7.46 (s, 2D), 7.25 (s, 3D); ^{13}C NMR (75 MHz, $CDCl_3$) δ 136.7 (s), 135.0 (s), 128.0 (t, J = 24.1 Hz), 127.9 (t, J = 24.4 Hz), 127.8 (t, J = 24.2 Hz), 89.5 (s); LRMS (EI) *m*/*z* 265 (M^+).

Benzophenone-d_{10}[3]

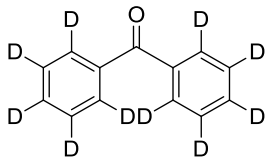

To a 250 mL round bottom flask was added: benzhydrol-d_{10} (6.08 g, 31.2 mmol) and CH_2Cl_2 (100 mL).[4] Pyridinium chlorochromate (6.73 g) followed by celite (10 g) was then added. Reaction was stirred at room temperature for 3 h. The solvent was evaporated to provide the crude material on celite. The mixture was purified by column chromatography (5:95 EtOAc/Hex) which afforded benzophenone-d_{10} as a light gold oil (4.63 g, 24.8 mmol, 80%). R_f = 0.52 (10% ethyl acetate in hexanes); ^{2}H NMR (46.1 MHz, CH_2Cl_2) δ 7.69 (s, 4D), 7.45-7.35 (m, 6D); ^{13}C NMR (75 MHz, $CDCl_3$) δ 196.7 (s), 137.3 (s), 131.9 (t, J = 23.8 Hz), 129.6 (t, J = 24.7 Hz), 127.7 (t, J = 24.0 Hz), 89.5 (s); IR (thin film, CH_2Cl_2) 3053, 2295, 2277, 1658, 1560 cm^{-1}; LRMS (CI, methanol) *m*/*z* 193 ([M+1]$^+$).

1,1,3-triphenylprop-2-yn-1-ol-d_{15}

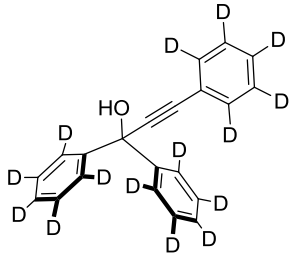

To a solution of (2,2-dibromovinyl)benzene-d_5 (5.79 g, 22.8 mmol) in dry THF (100 mL) at -78 °C was added 2.5 M *n*-BuLi in hexanes (10.4 mL, 26.0 mmol). The mixture stirred for 3 hours warming to room temperature. The reaction was cooled to 0 °C, then benzophenone-d_{10} (2.50 g, 13.0 mmol) was added dropwise as a solution in THF (10 mL) and the reaction mixture was allowed to warm to room temperature. The reaction mixture was stirred for another 18 hours. The mixture was quenched by addition of 6% aq. NH_4Cl (50 mL) and the resulting mixture was extracted with diethyl ether (50 mL). The organic extracts were washed with brine (3 × 50 mL) and dried over Na_2SO_4. After filtration, removal of the solvent under reduced pressure gave the crude product. The product was purified by column chromatography using a slow gradient from hexanes to 20% ethyl acetate in hexanes providing 1,1,3-triphenylprop-2-yn-

1-ol-d_{15} as a white solid (5.39 g, 18.7 mmol, 82%). R_f = 0.32 (1:4 EtOAc/Hex); ^{1}H NMR (300 MHz, $CDCl_3$) δ 2.87 (s, 1 H); ^{2}H NMR (46.1 MHz, CH_2Cl_2) δ 7.76 (s, 4D), 7.50 (s, 2D), 7.30 (s, 9D); ^{13}C NMR (75 MHz, $CDCl_3$) δ 144.8, 131.2 (app d, J = 25.0 Hz), 128.0 (app t, J = 25.4 Hz), 125.6 (t, J = 24.0 Hz), 122.1 (s), 91.6 (s), 87.1 (s), 77.2 (s), 74.7 (s), 48.0 (s); IR (thin film, CH_2Cl_2) 3553, 3447, 3051, 1563 cm^{-1}; LRMS (EI) m/z 282 (M^+); mp 81–83 °C.

1,1,3-triphenylprop-2-yn-1-ol-d_{16}

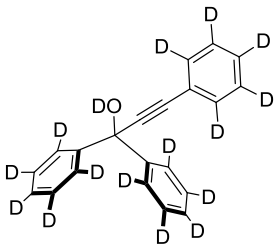

A 100 mL round bottom flask was charged with 1,1,3-triphenylprop-2-yn-1-ol-d_{15} (5.39 g, 18.7 mmol), CH_2Cl_2 added until material dissolved, then added equal amount of D_2O. The mixture was stirred for 30 min. The layers were separated and the organic layer was dried over Na_2SO_4, filtered, and concentrated to give 1,1,3-triphenylprop-2-yn-1-ol-d_{16} (4.86 g, 16.2 mmol, 86%) Deuterium incorporation was confirmed by ^{1}H NMR (OH peak disappearance).

5,6,11,12-tetraphenyltetracene-d_{28} (rubrene-d_{28})

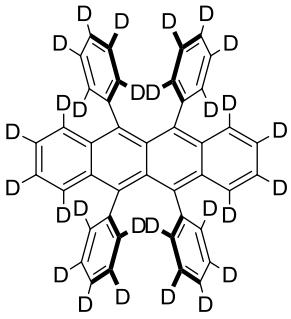

To a solution of 1,1,3-triphenylprop-2-yn-1-ol-d_{16} (4.50 g, 15.0 mmol) in 64 mL of toluene-d_8 was added distilled TEA (3.14 mL, 22.5 mmol). The mixture was cooled to 0 °C and methane sulfonyl chloride (1.74 mL, 22.5 mmol) was added dropwise. The reaction was stirred at 0 °C for 15 min, at room temperature for 30 min, then was heated at 110 °C for 6 hours. Upon cooling, the mixture was diluted with 40 mL of ethyl acetate, transferred to a separatory funnel, and washed with 2 M HCl (3 × 40 mL). The organic layer was dried over $MgSO_4$ and the solvent was removed *in vacuo*. The residue was diluted with a diethyl

ether/methanol solution (1:1). Filtration provided 5,6,11,12-tetraphenyltetracene-d_{28} as a red-orange solid (0.444 g, 0.792 mmol, 5%, 97.2% deuterium). R_f = 0.51 (1:3 Benzene/Hex); ^{2}H NMR (46.1 MHz, CH_2Cl_2) δ 7.11 (sb, 28D); ^{13}C NMR (75 MHz, $CDCl_3$) δ 141.6 (s), 136.9 (s), 131.6 (t, J = 24.4 Hz), 130.2 (s), 129.1 (s), 126.7 (t, J = 22.9 Hz), 126.4-125.9 (m), 125.2 (t, J = 23.2 Hz), 124.3 (t, J = 21.4 Hz); IR (KBr pellet) 2266, 1610, 1565 cm^{-1}; HRMS (ESI) calcd for $[C_{42}D_{28}]^+$ 560.3948, found 560.3949; Anal. calcd for $C_{42}D_{28}$: C, 89.94; D, 10.06 (seen as H, 5.30). Found: C, 89.93; H, 4.97. mp 322–326 °C.

2. Spectral data

Parameter	Value
1 Data File Name	C:/ Users/ Katie/ Desktop/ D28_FIDs/ FIDs/ Bromovinylbenzene_1H.fid/ fid
2 Solvent	cdcl3
3 Acquisition Date	2010-11-02T21:24:14
4 Spectrometer Frequency	300.17
5 Nucleus	1H

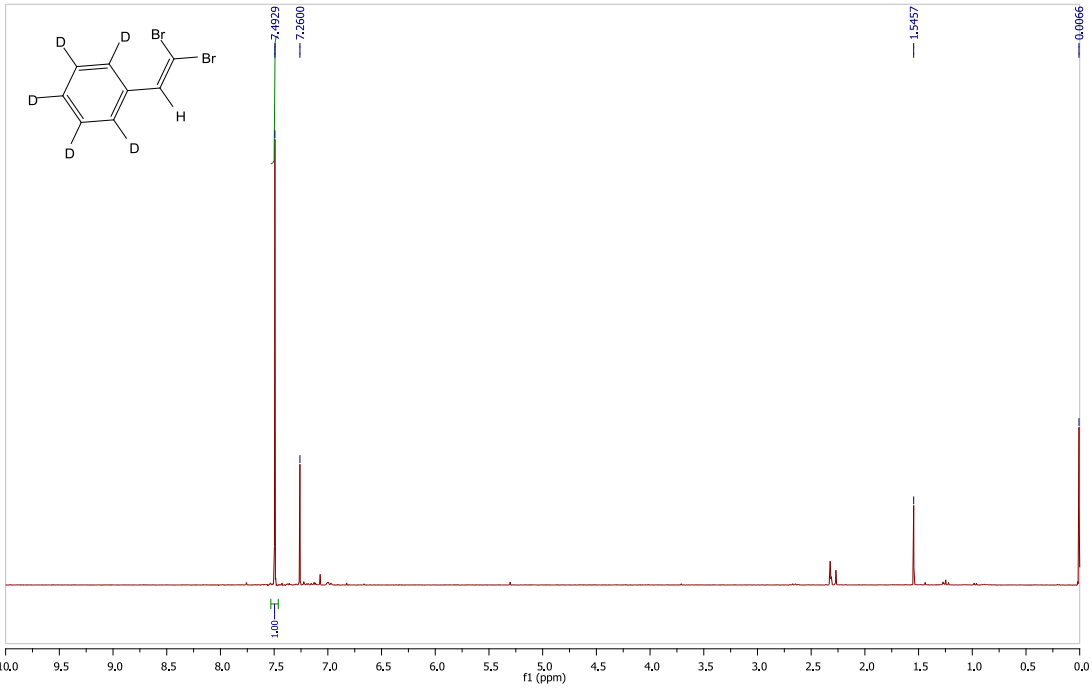

Parameter	Value
1 Data File Name	C:/ Users/ Katie/ Desktop/ D28_FIDs/ FIDs/ Bromovinylbenzene_2H.fid/ fid
2 Solvent	c6d6
3 Acquisition Date	2009-07-08T16:39:19
4 Spectrometer Frequency	46.08
5 Nucleus	2H

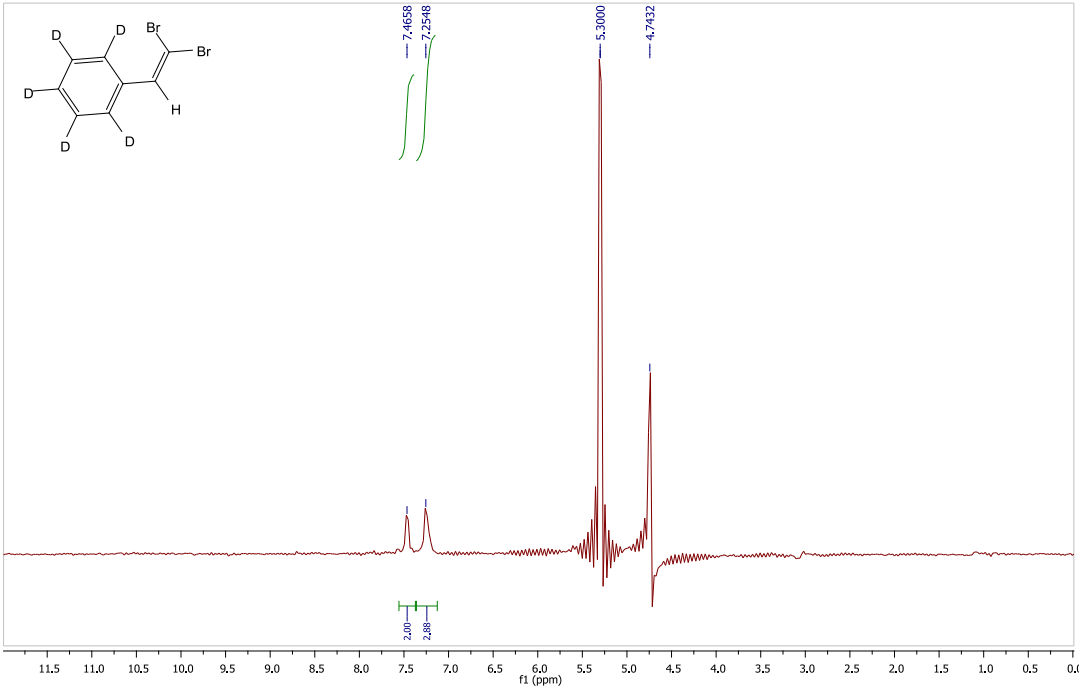

Parameter	Value
1 Data File Name	C:/ Users/ Katie/ Desktop/ D28_FIDs/ FIDs/ Bromovinylbenzene_13C.fid/ fid
2 Solvent	CDCl3
3 Acquisition Date	2009-07-22T06:34:30
4 Spectrometer Frequency	75.43
5 Nucleus	13C

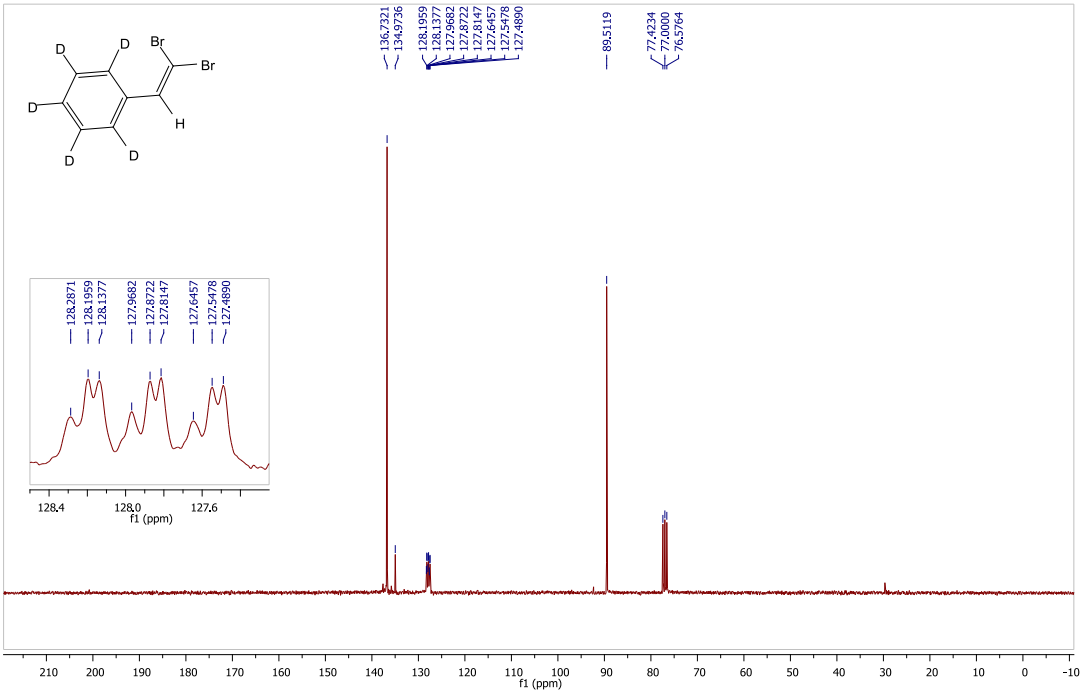

Parameter	Value
1 Data File Name	C:/ Users/ Katie/ Dropbox/ ChemResearch/ NMR data/ dRubrene/ Files_022613/ KAMI-73-1.fid/ fid
2 Solvent	cdcl3
3 Acquisition Date	2009-06-24T21:24:43
4 Spectrometer Frequency	300.17
5 Nucleus	1H

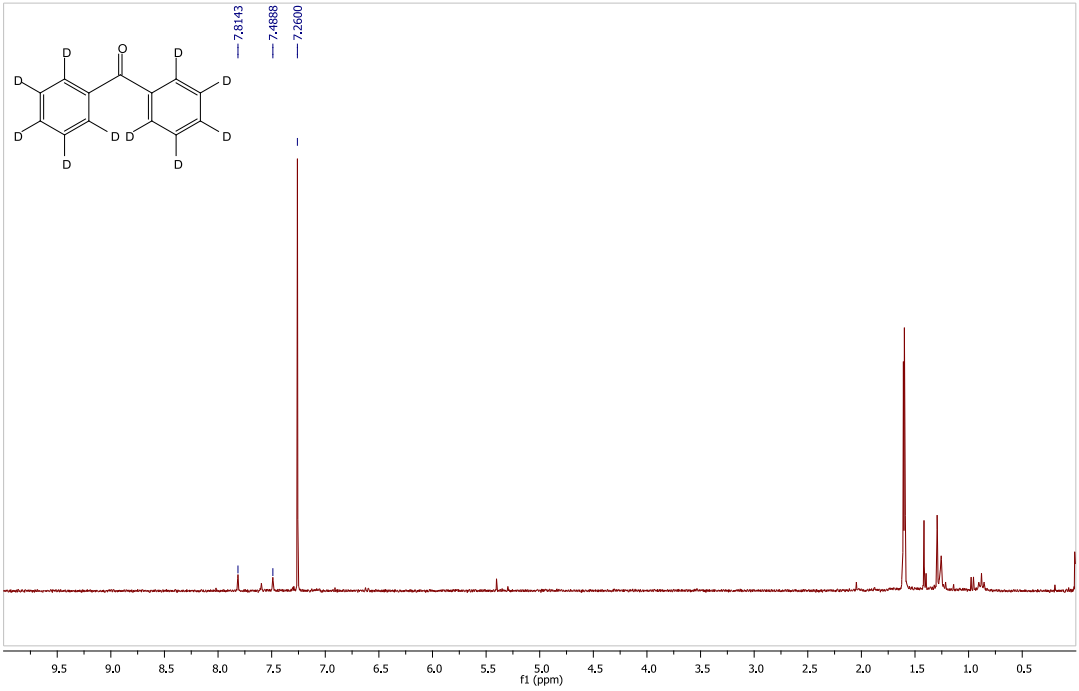

Parameter	Value
1 Data File Name	C:/ Users/ Katie/ Dropbox/ ChemResearch/ NMR data/ dRubrene/ Files_022613/ KAMI-73-2H.fid/ fid
2 Solvent	c6d6
3 Acquisition Date	2009-06-25T20:52:35
4 Spectrometer Frequency	46.08
5 Nucleus	2H

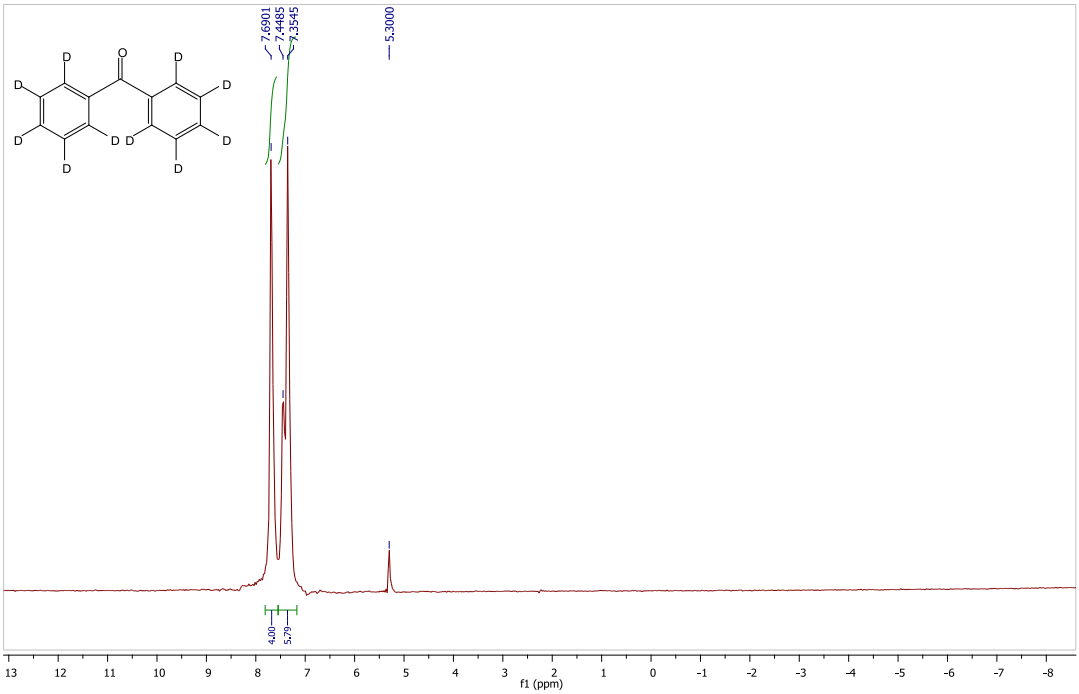

Parameter	Value
1 Data File Name	C:/ Users/ Katie/ Dropbox/ ChemResearch/ NMR data/ dRubrene/ Files_022613/ 090719v3_0603.fid/ fid
2 Solvent	CDCl3
3 Acquisition Date	2009-07-19T23:13:00
4 Spectrometer Frequency	75.43
5 Nucleus	13C

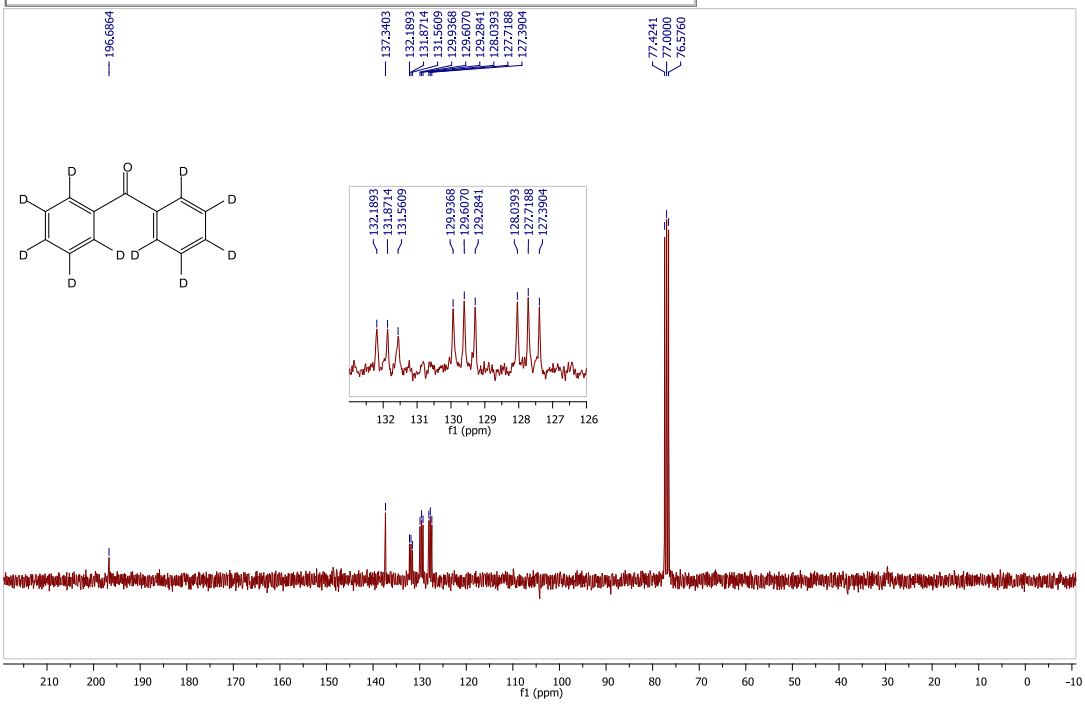

Parameter	Value
1 Data File Name	C:/ Users/ Katie/ Desktop/ D28_FIDs/ FIDs/ propargylalcohol_1H.fid/ fid
2 Solvent	cdcl3
3 Acquisition Date	2010-04-13T19:15:16
4 Spectrometer Frequency	300.17
5 Nucleus	1H

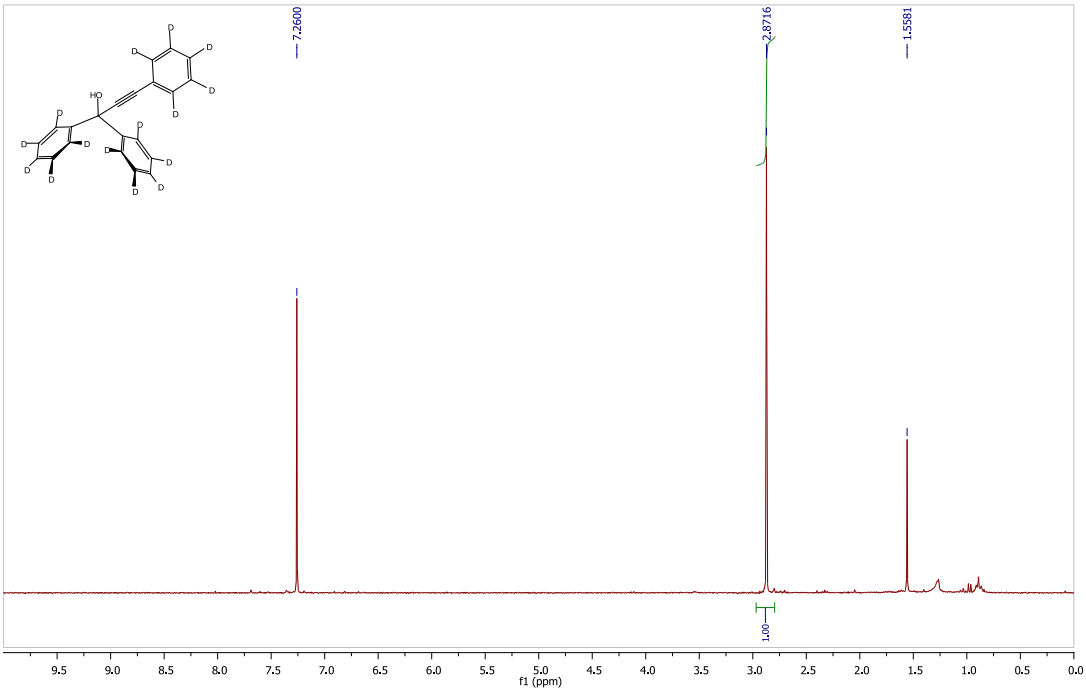

Parameter	Value
1 Data File Name	C:/ Users/ Katie/ Desktop/ D28_FIDs/ FIDs/ propargylalcohol_2H.fid/ fid
2 Solvent	c6d6
3 Acquisition Date	2009-07-08T16:30:59
4 Spectrometer Frequency	46.08
5 Nucleus	2H

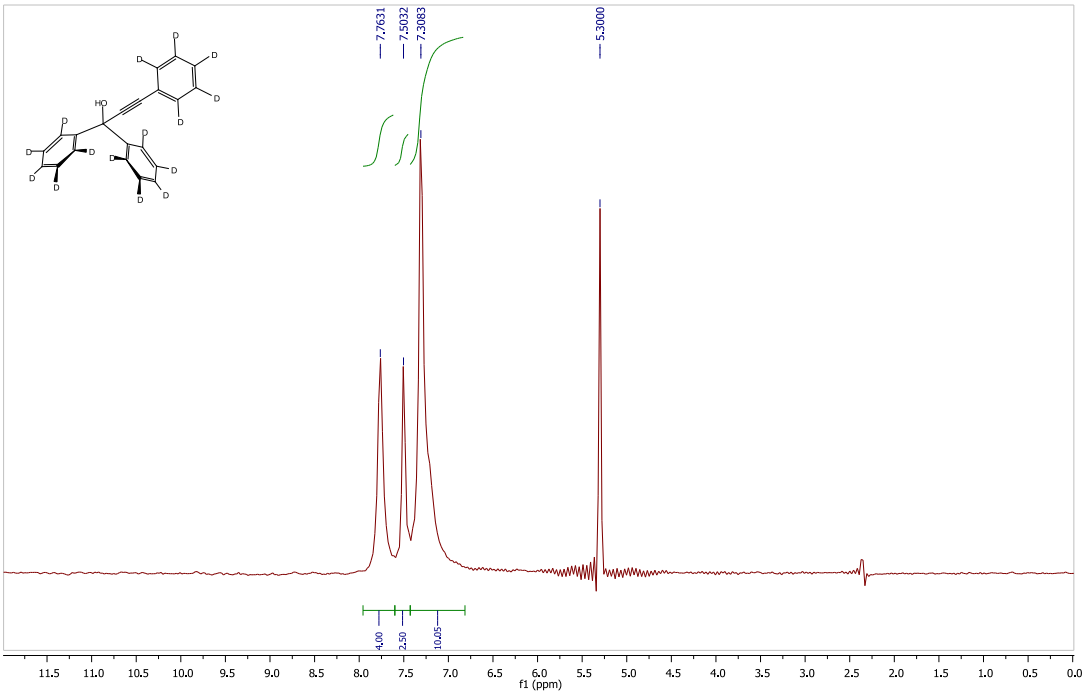

Parameter	Value
1 Data File Name	C:/ Users/ Katie/ Desktop/ D28_FIDs/ FIDs/ propargylalcohol_13C.fid/ fid
2 Solvent	CDCl3
3 Acquisition Date	2009-08-19T09:26:45
4 Spectrometer Frequency	75.43
5 Nucleus	13C

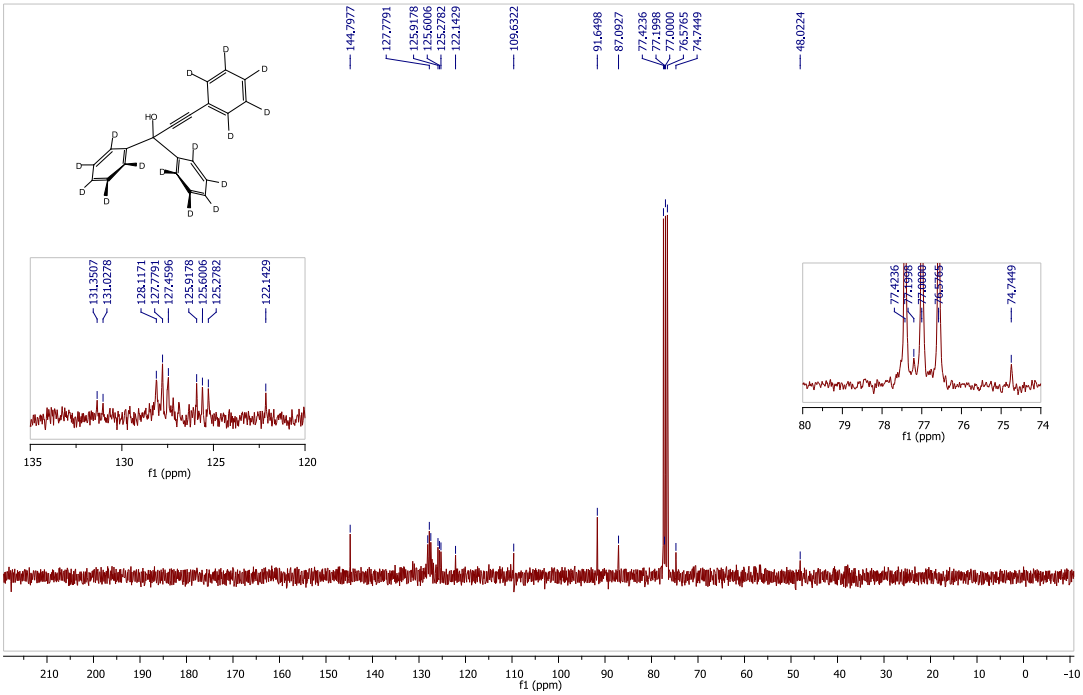

Parameter	Value
1 Data File Name	C:/ Users/ Katie/ Desktop/ D28_FIDs/ FIDs/ D28rubrene_1H/ fid
2 Solvent	CDCl3
3 Acquisition Date	2012-12-06T15:18:15
4 Spectrometer Frequency	500.13
5 Nucleus	1H

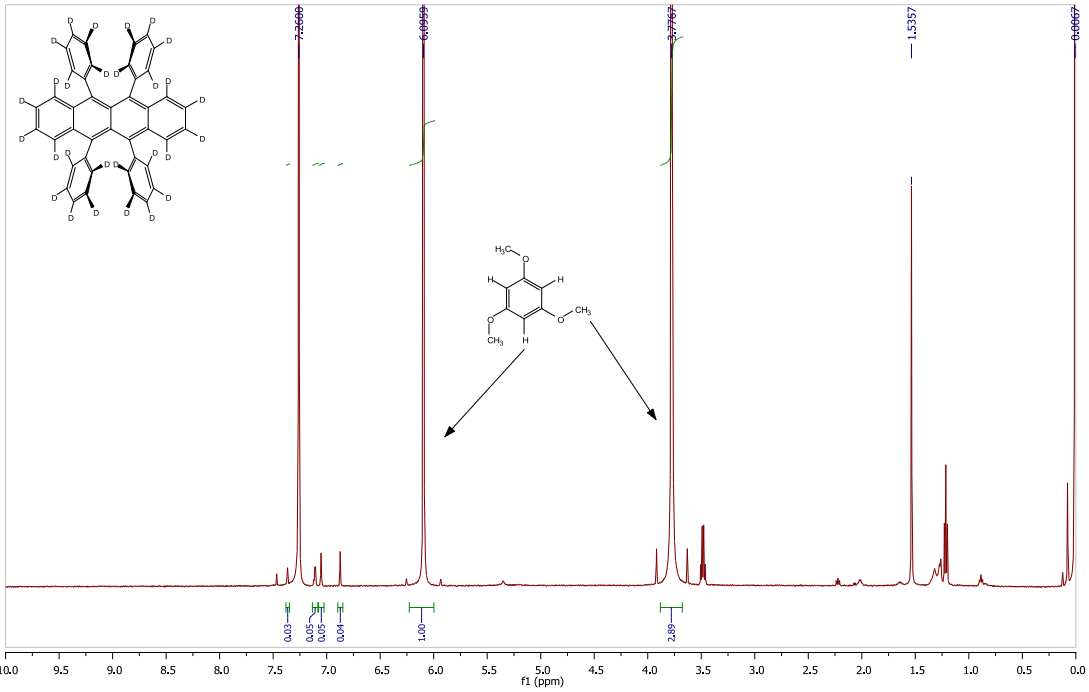

Parameter	Value
1 Data File Name	C:/ Users/ Katie/ Desktop/ D28_FIDs/ FIDs/ D28rubrene_2H.fid/ fid
2 Solvent	c6d6
3 Acquisition Date	2009-07-08T17:49:01
4 Spectrometer Frequency	46.08
5 Nucleus	2H

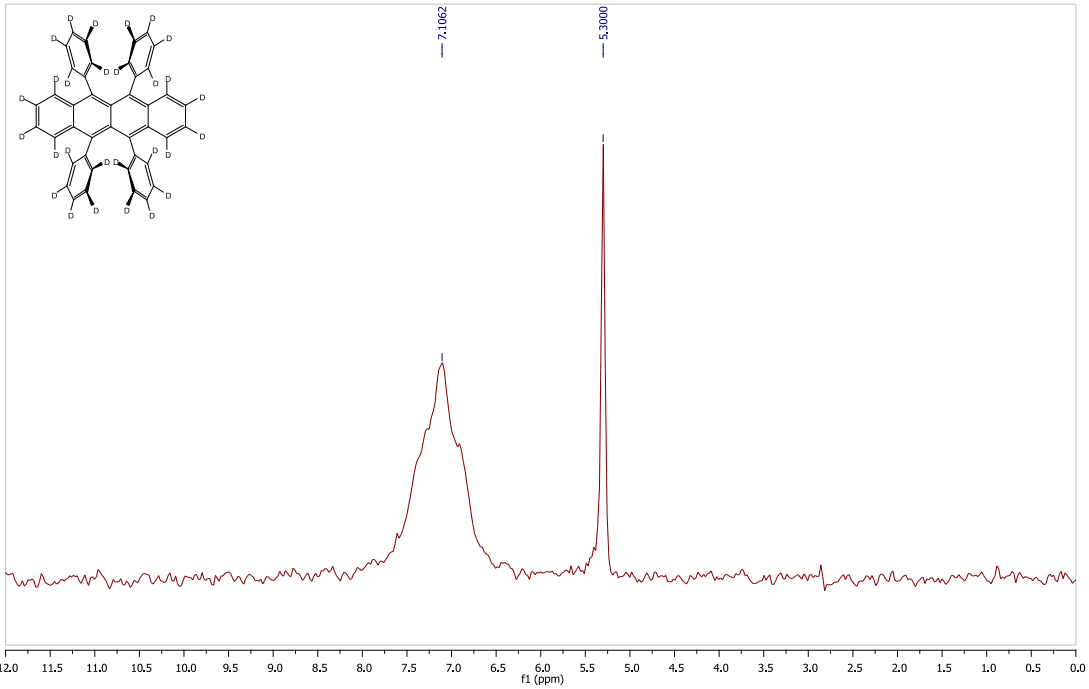

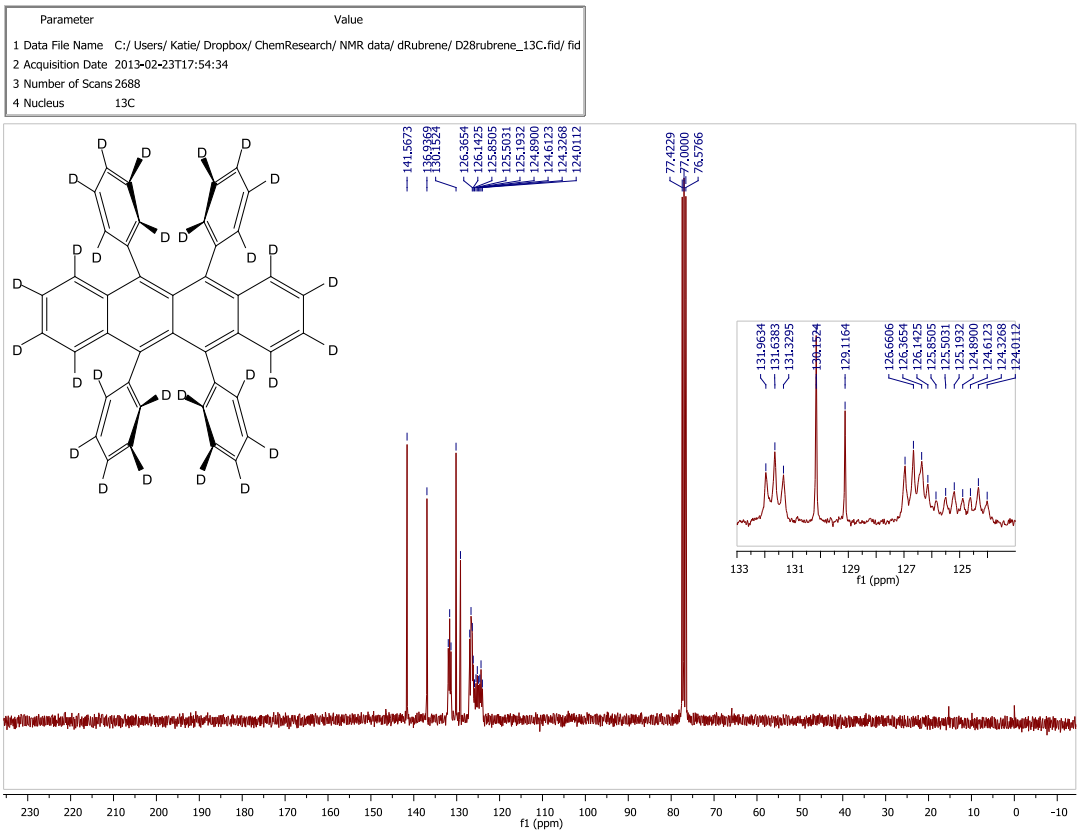

3. Electrical characterization of H-rubrene vacuum-gap FETs

In order to understand the isotope effect in the charge transport of rubrene single crystals, we carried out a systematic electrical measurement of H-rubrene vacuum-gap FETs at variable temperatures, in comparison with the results obtained in D-rubrene crystals. The purification, crystal growth, device fabrication and electrical measurements of H-rubrene crystals were performed in the same way as in D-rubrene crystals, as discussed in the text.[5–7] From Figure S1(a), we found that the temperature dependence of mobility for H-rubrene crystals was similar to what D-rubrene crystals exhibited, namely, the transport behavior was strongly sample-dependent. In the best case in Sample A, mobility reached 42 $cm^2V^{-1}s^{-1}$ at lower temperatures with $T^* \leq 87$ K. Sample B had a slightly lower mobility at low temperatures, around 30 $cm^2V^{-1}s^{-1}$, but the activated transport regime was still not observed down to 90 K. In Sample C, we observed the transition from bandlike to activated transport at T^* = 150 K. Despite these

observations, a direct correlation between mobility and threshold voltage (shown on Figure S1(b)), could not be established. Nevertheless, these measurements have confirmed that replacing protons with deuteriums in rubrene crystals does not have a traceable impact on the electrical transport behaviors, such as the magnitude of the mobility and its temperature dependence. The isotope effect, as we have pointed out in the introduction, more likely plays an important role in modifying the spin response in organic spin valve devices.[8] We also note that although our results in H-rubrene crystals (vacuum-gap structure) are qualitatively consistent with Podzorov's report, we have achieved higher low-temperature mobility and a broader temperature range in which bandlike transport occurs, compared with their observations.[6] We speculate that this is likely related to the higher purity of our H-rubrene crystals, since extensive purification is an effective strategy to improve the carrier mobility.[9]

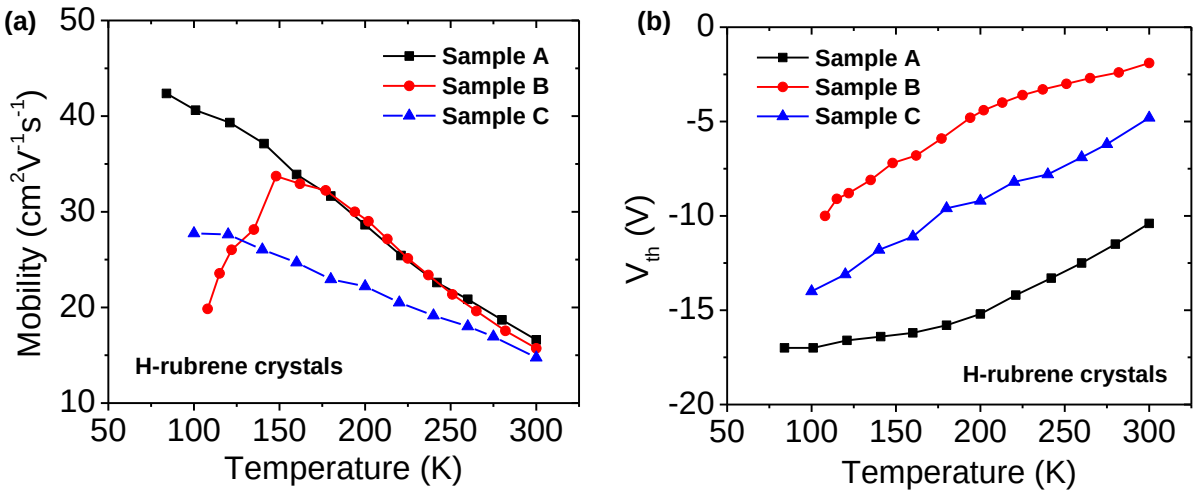

Figure S1. Temperature dependence of mobility **(a)** and threshold voltage **(b)** in H-rubrene single crystal vacuum-gap FETs. Results from three representative samples are shown here. Parameter extraction is based the method described in the main text.

4. Modeling of the temperature dependence of mobility and threshold voltage

To understand the temperature dependence of mobility and threshold voltage in D-rubrene vacuum-gap FETs, we applied a carrier trapping model developed by Morpurgo *et al* to our experimental data.[10] In this model, charge transport in highly order molecular crystals is assumed to occur in band states. Specifically for hole-transporting crystals, only those carriers move in the valence band (with density of states (DOS) N_0 for energy $E > 0$) contribute to channel conduction. N_0 is taken to be about 10^{15} $cm^{-2}eV^{-1}$ by dividing the molecular density at the surface by the bandwidth (~ 0.5 eV). The boundary between delocalized band states and localized trap states is known as the mobility edge, assumed to be a sharp edge located at $E = 0$. At $E < 0$, disordered-induced trap states exist, consisting of shallow trap states with DOS $N_S(E)$ located at a few k_BT away from mobility edge and deep traps with DOS $N_D(E)$ at further deep into the band gap. The mobility of carriers moving in the band is the intrinsic mobility of the material, and it depends on the temperature as $\mu_0(T) = \alpha T^2$, in which α is a material-dependent-only parameter. Carriers occupying the trap states do not contribute to channel current.

We can use either a constant distribution of shallow traps ($N_S(E) = N_C$ = constant if $E_C < E < 0$, and $N_S(E) = 0$ otherwise), or a Gaussian distribution ($N_S(E) = N_g e^{-(E/2E_g)^2}$). For the deep traps, we use a "square" distribution ($N_D(E) = N_D$ = constant if $E_D - \delta E_D/2 < E < E_D + \delta E_D/2$ and zero otherwise). For a given trap DOS, we calculate the position of Fermi level E_F numerically as a function of temperature (T) and total charge density ($n = C_i V_G$) through the relation

$$n = n_f + n_t = \int_0^{+\infty} N_0 \frac{1}{e^{(E-E_F)/k_BT}} dE + \int_{-\infty}^{0} [N_S(E) + N_D(E)] \frac{1}{e^{(E-E_F)/k_BT}} dE \quad (1)$$

Once determining $E_F(T, n)$, we can then obtain the drain current I_D using the density of charge carriers occupying the band states (free carrier density), which is $n_f(n,T) = \int_0^{+\infty} N_0 \frac{1}{e^{(E-E_F)/k_BT}} dE$, through

$$I_D(n) = n_f(n,T) e \mu_o(T) \frac{W}{L} V_D \quad (2)$$

From Equation (2), we can extract all quantities that are measured experimentally, such as mobility $\mu(T)$ and threshold voltage $V_{th}(T)$, using the same extraction methods as discussed in the main text. Specifically, $V_{th}(T)$ is obtained by the intercept of linear extrapolation of I_D to V_G-axis, and $\mu(T)$ is from $\mu(T) = \mu_0(T) \frac{\partial n_f(n,T)}{\partial n} \propto \frac{\partial I_D}{\partial V_G}$. The value of α is set the same for different trap distributions, since it is only dependent on the materials properties. This leaves only two fitting parameters (height and width of the tail states), namely, N_C and E_C or N_g and E_g for fitting $\mu(T)$ depending on which shallow trap distribution, and N_D and E_D for fitting of $V_{th}(T)$. This model has been used to analyze the temperature dependence of mobility in high performance single crystals of p-type TMTSF and n-type PDIF-CN_2.[10,11]

References

(1) Greene, A. K.; Scott, L. T. *J. Org. Chem.* **2012**, Article ASAP.

(2) Corey, E. J.; Fuchs, P. L. *Tetrahedron Lett.* **1972**, *13*, 3769–3772.

(3) Zheng, C.; Hofstetter, H.; Hofstetter, O. *J. Mol. Struct.* **2008**, *875*, 173–182.

(4) Li, H.; Zhu, R.-Y.; Shi, W.-J.; He, K.-H.; Shi, Z.-J. *Org. Lett.* **2012**, *14*, 4850–4853.

(5) Laudise, R. A.; Kloc, C.; Simpkins, P. G.; Siegrist, T. *J. Cryst. Growth* **1998**, *187*, 449–454.

(6) Podzorov, V.; Menard, E.; Borissov, A.; Kiryukhin, V.; Rogers, J. A.; Gershenson, M. E. *Phys. Rev. Lett.* **2004**, *93*, 86602.

(7) Menard, E.; Podzorov, V.; Hur, S. H.; Gaur, A.; Gershenson, M. E.; Rogers, J. A. *Adv. Mater.* **2004**, *16*, 2097–2101.

(8) Nguyen, T. D.; Hukic-Markosian, G.; Wang, F.; Wojcik, L.; Li, X. G.; Ehrenfreund, E.; Vardeny, Z. V. *Nat. Mater.* **2010**, *9*, 345–352.

(9) Bisri, S. Z.; Takenobu, T.; Takahashi, T.; Iwasa, Y. *Appl. Phys. Lett.* **2010**, *96*, 183304–183304.

(10) Xie, H.; Alves, H.; Morpurgo, A. F. *Phys. Rev. B* **2009**, *80*, 245305.

(11) Minder, N. A.; Ono, S.; Chen, Z.; Facchetti, A.; Morpurgo, A. F. *Adv. Mater.* **2012**, *24*, 503–508.